ASIAN JOURNAL OF CIVIL ENGINEERING (BUILDING AND HOUSING) VOL. 13, NO. 2 (2012)
PAGES 181-193

AN INVESTIGATION ON THE SEISMIC PERFORMANCE OF REINFORCED CONCRETE PANEL STRUCTURES

B. Hassani[*a] and A. Jafari[a]
[a]Department of Civil Engineering, Shahrood University of Technology, Shahrood, Iran

Received: 5 January 2011; **Accepted:** 8 July 2011

ABSTRACT

An investigation on the seismic performance of panel structures with permanent shuttering system is the subject of this article. Three building models with similar plan and different heights are taken into consideration. The nonlinear behavior of these structures are studied by PERFORM 3D software and its multi-layer shell finite elements with fiber sections. Carrying out the analysis, the performance level of each model is determined. According to the obtained results, it is concluded that the performance level of the structures which are designed based on the common codes is higher than their pre assumption, i.e. life safety.

Keywords: Panel buildings; performance level; nonlinear behavior; shear wall; nonlinear static analysis

1. INTRODUCTION

The recent advances in using concrete panel construction technology have been growing in recent years. One of the common methods is the so named permanent shuttering system which indeed is a pre-formed panel construction technique. In this approach, the shuttering and most of the reinforcing are carried out in the factory by using polystyrene panels. Besides acting as the formwork for concrete casting, these panels also act as thermal insulators. It should be noted that in the panel building structures, most of the time the conventional frame elements, i.e. beams and columns, do not exist and all of the gravitational and lateral loads are resisted by a system comprising slabs and panel walls.

Different studies on the damages caused by earthquakes indicates that although in most of the buildings designed based on the current codes of practice, the total performance from a life saving point of view is quite acceptable, however, the overall damage is relatively high. It seems that a remedy for this problem is to take into consideration different levels of performance in the design procedure. By this approach, one would be able to design a building in such a way that certain levels of performance can be expected for different levels of hazard [1].

[*] E-mail address of the corresponding author: b_hassani@iust.ac.ir (B. Hassani)

Although some research can be found in the literature which study the behavior of the sandwich panel structures, but a very few is available on the buildings constructed of the permanent shuttering concrete panels. In this research, to study the levels of performance of typical buildings, which are designed based on the currently practiced codes, three different panel buildings are considered, Figure 1. These structural models are common in plan but vary in height. The considered plan layouts are symmetric in both directions and are comprised of coupled walls in the form of 'T' and 'L' shapes which have different deformation capacities.

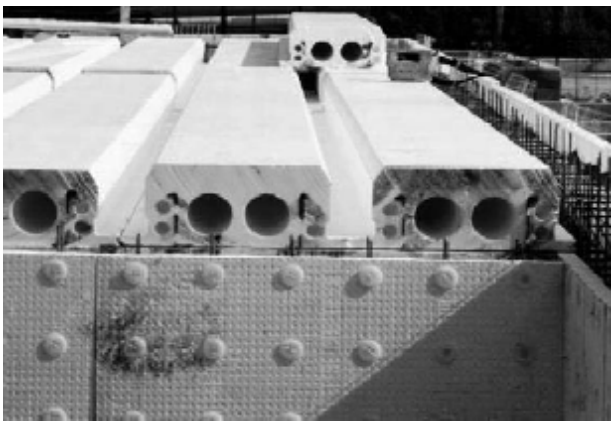

Figure 1. Wall and one way slab construction with permanent shuttering system

2. **MODELING FOR NONLINEAR BEHAVIOR**

For providing a proper model to consider the nonlinear behavior of the shear walls the instructions of FEMA 273 [2] is used. According to this guideline, based on the ratio of height to length of shear walls, (H/L), two different types of nonlinear behavior are realized: controlled by flexure and controlled by shear.

In this research, three different models are considered where all have a similar square plan with a dimension of 12 m in both directions, as is illustrated in Figure 2. The structural system is assumed to be bearing walls comprised of concrete shear walls. The heights of these models are considered to be 20, 30 and 40 m, in 6, 9 and 12 stories, respectively. It should be noted that the height of the third model is 10 m more than the maximum suggested by Iranian Seismic Code (ISC) [3] which is similar to UBC-94 [4]. The height of the coupling spandrel beams in all of these models is taken equal to 1.2 m. The widths of the openings in two directions are different and in the H2 direction, as shown in Figure 2, are twice as much of H1. Since the ratios of height to length (H/L) for all of bearing walls of the studied models are greater than 3, they are slender and their nonlinear behavior is controlled by flexure. Therefore, their behavior against shear can be considered as linear.

To obtain a more realistic estimation for behavior of the considered models, instead of the commonly practiced equivalent beam-column models [5], here a finite element model with multi-layered shell elements is employed that is able to take into account the cracking of the concrete and consequently shifting of the neutral axis of the flexural members. In

order to define the cross section of each layer that is used in PERFORM 3D software, the so named fiber sections are used. By using these fiber sections the cross sections of elements are described and a non-linear behavior modeling is constructed.

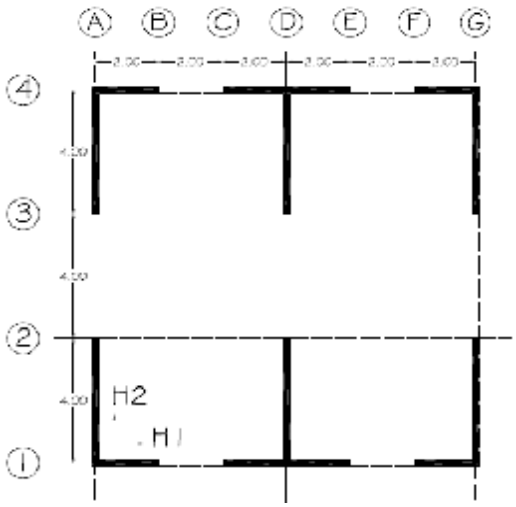

Figure 2. Plan of the models

Modeling of the cross section of each element should be done by an adequate arrangement of steel and concrete fibers. The behavior of the fibers has been defined using stress-strain curves with a high level of accuracy. Each element, which is considered as a layer, describes one of the mechanical characteristics of reinforced concrete, Figure 3. To model the behavior of concrete shear walls, several layers are employed which are joined in a parallel fashion.

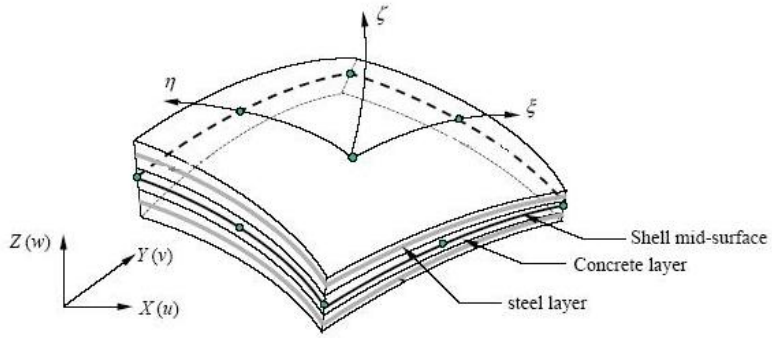

Figure 3. Finite element model with multi-layered shell elements

After modeling and analysis of the models, the demand capacity ratios (DCR) have been calculated by making use of the rotation gage elements and finally the performance level of each model is determined. To model nonlinear behavior of slender wall among available elements in software library, ‘shear wall element’ is employed. The combination of two axial-bending and shear layers models flexure and shear behavior in these walls. These layers are joined in the nodes of elements and behave as parallel layers [6].

In this research three kinds of layers has been employed including:

a. The concrete axial-bending layer
b. The steel axial-bending layer
c. The concrete shear layer

Both concrete and steel axial-bending layers are employed to model flexural and axial behavior and the concrete shear layer is employed to model shear behavior. The fibers of both concrete and steel axial-bending layers have been vertically placed and behavior of the walls in two other directions including horizontal and out of plane directions assumed elastic. Due to the arrangement of reinforcements in the panels of permanent shuttering system, it is impossible to construct boundary elements in edges or wall intersections. Therefore, the concrete fibers used in concrete axial-bending layers are considered as unconfined concrete.

2.1 Characteristics of concrete fibers

The phenomena such as crushing and cracking which often happen in loading concrete segments, cause nonlinear behavior in concrete. Modeling nonlinear behavior in concrete is very complicated and choosing a suitable model that can describe the nonlinear behavior needs a good knowledge and experience. As it is shown in Figure 4, the uniaxial stress-strain curve of unconfined concrete is comprised of two parts. First, ascending part of the curve to maximum compressive strength (f_c') which is defined by Equation (1) suggested by Saenz

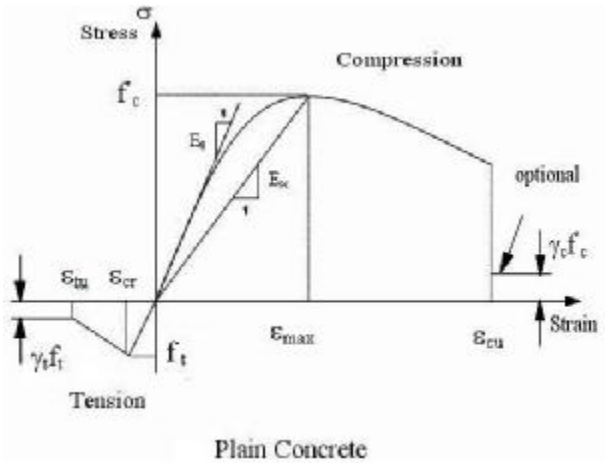

4. Uniaxial stress-strain curve of concrete fibers

$$s = \frac{E_0 e}{1+\left(\frac{E_0}{E_{SC}}-2\right)\left(\frac{e}{e_{\max}}\right)+\left(\frac{e}{e_{\max}}\right)^2} \tag{1}$$

where E_0 is the initial modulus of elasticity and E_{sc} is the secant modulus in maximum stresses and s is stress nd e is strain and $e_{\max}$ is strain in the maximum stress [7]. Then the descending part of curve is defined by the model suggested by Smith and Young [8]:

$$s = s_c \left(\frac{e}{e_{\max}} \right) e^{\left(1 - \frac{e}{e_{\max}}\right)} \quad (2)$$

where s_c is the compressive strength of concrete and when the concrete specimen loading is uniaxial, this parameter (s_c) equals f_c'. In order to prevent creating errors in calculations after crushing ($e > e_{cu}$) and concrete cracking ($e > e_{tu}$) a very small amount of tensile and compressive stress is determined by $g_t f_t'$ and $g_c f_c'$ (Figure 4). It should be mentioned that tensile strength of concrete fibers is ignored in this research.

2.2 Modeling of cracking phenomenon

For modeling the cracking phenomenon in wall sections considering the points which have high cracking potential, i.e. wall edges, the area of the fibers in these points are considered much more smaller than other points. Therefore, the fibers which are located on the edges of these walls rupture sooner. As a result, cracking phenomenon and shifting of the neutral axis are being modeled with high accuracy.

2.2.1 The concrete shear layer

The third layer which is used for modeling the wall elements is called the concrete shear layer. The fibers are not used in constructing such a wall. In this research, shear behavior in walls is assumed elastic and for defining this layer, the two parameters, shear modulus (G) and shear strength (v_c), are used. In estimating shear strength (v_c) according to FEMA 273 guideline the methods which are mentioned in ACI 318-05 are used and the amount of the shear strength (v_c) in this layer is taken as $25\,kg/cm^2$ [9-10]. For estimating the magnitude of shear modulus (G), with the assumption of $v = 0.25$, the common assumption of $G = 0.4E$ for the cracked concrete is too high. Therefore the shear modulus (G) is assumed to be 0.25 times of this value [11].

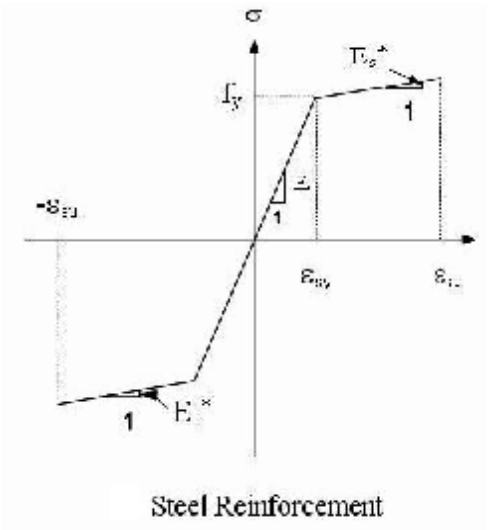

Figure 5. Uniaxial stress-strain curve of steel fibers

2.2.2 Characteristics of steel fibers

Steel reinforcements, as shown in Figure 5, are being modeled like an elastic material with strain hardening. In this layer, the distribution of steel fibers is uniform which is similar to the distribution of reinforcements in concrete panels.

2.3 Hinge region in walls

According to the guideline FEMA 273 [2], since the nonlinear behavior of the shear walls is controlled by flexure, the rotation above the hinge region, which is located at the end of the member, is the criterion for assessing this behavior. In this research, for evaluating the rotation in walls, rotation gage elements are used. These are four-node elements that are connected to one or a group of wall elements and their height is measured according to the length of the hinge region. Since the rotation in the hinge region is proportional to the height of the hinge region, estimating the height of this region is the most important factor in evaluating the rotation of the walls. FEMA 356 [9] recommends a hinge length equal to the smaller of (a) one half the cross section depth and (b) the story height. In determining the length of the hinge region, if the stiffness of the coupling spandrel beams is too high, the length of the wall can be assumed as the sum of the lengths of the coupling walls. However since in all of the models the stiffness of the coupling spandrel beams is low, the length of each wall in every direction is taken into consideration separately.

3. PUSH-OVER ANALYSIS

After nonlinear modeling, for assessing the performance level, the models are being analyzed. The analysis which is used in this research is nonlinear static analysis and after these analyses the push-over curves are drawn. In these curves, the X axis is the reference displacement, usually displacement of roof, and the Y axis is the horizontal load. By using the push-over curves, the performance levels of these specimens are determined. Since the result of these push-over analyses change according to the lateral load pattern, three types of loading are defined in this article:

Equivalent Lateral Force (ELF): a lateral load pattern represented by values of *Cvx* given in FEMA 273 [2], which may be used if more than 75% of the total mass participates in the fundamental mode in the direction under consideration.

Modal Compatible Distribution (MCD): a lateral load pattern proportional to the story inertia forces consistent with the story shear distribution calculated by combination of modal responses using response spectrum analysis of the building including a sufficient number of modes to capture 90% of the total mass.

Uniform Load Distribution (ULD): often termed the uniform pattern, based on lateral forces that are proportional to the total mass at each floor level.

In combining gravity and seismic loads, the effect of the gravity loads is considered in two ways:

a) When the effects of gravity counteract seismic loads:

$$Q_{G1} = 0.9\, Q_D \tag{3}$$

b) When the effects of gravity and seismic loads are additive:

$$Q_{G2} = 1.1(Q_D + Q_L) \tag{4}$$

It should be noted that the analyses in this research are based on the displacement control method where we have specified the displacement increment is instead of the load increment. The obtained push-over curves for different load patterns in each of the main directions are illustated in Figures 6-11.

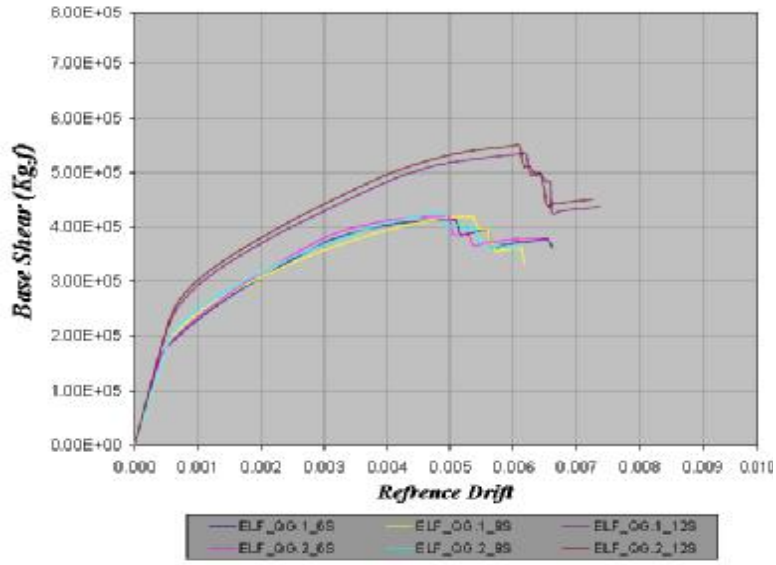

Figure 6. Push-over curves of the ELF load pattern in H1 direction

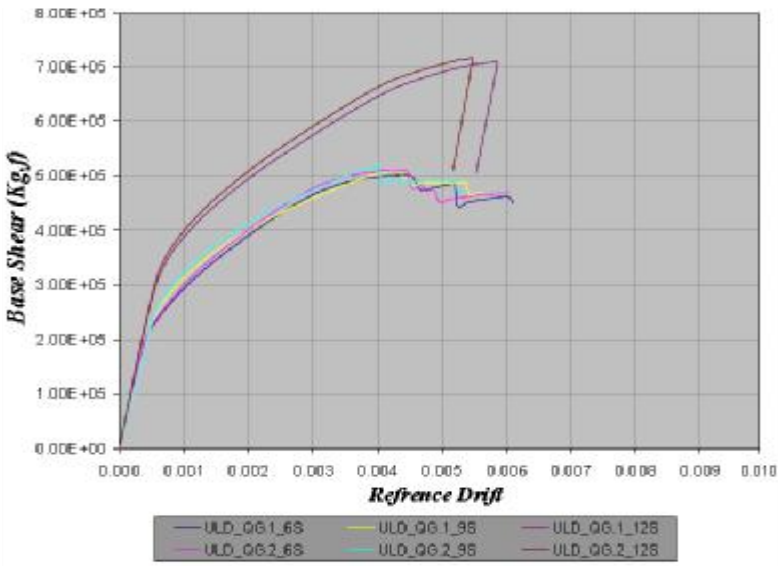

Figure 7. Push-over curves of the ULD load pattern in H1 direction

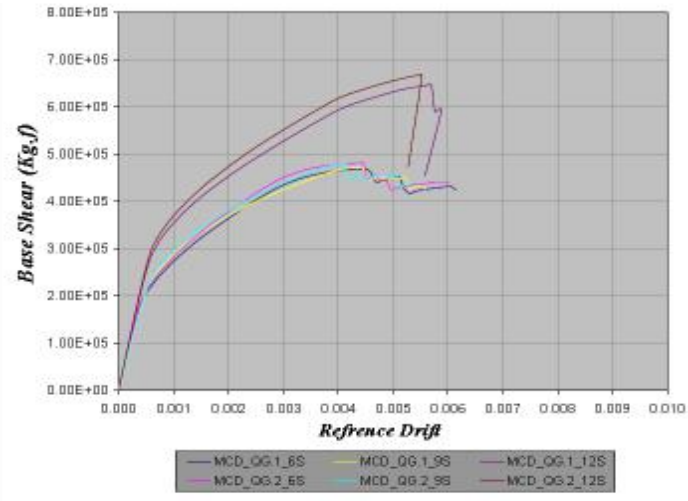

Figure 8. Push-over curves of the MCD load pattern in H1 direction

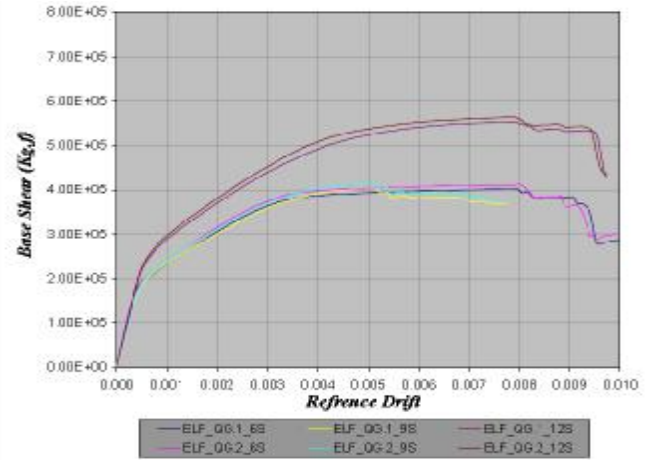

Figure 9. Push-over curves of the ELF load pattern in H2 direction

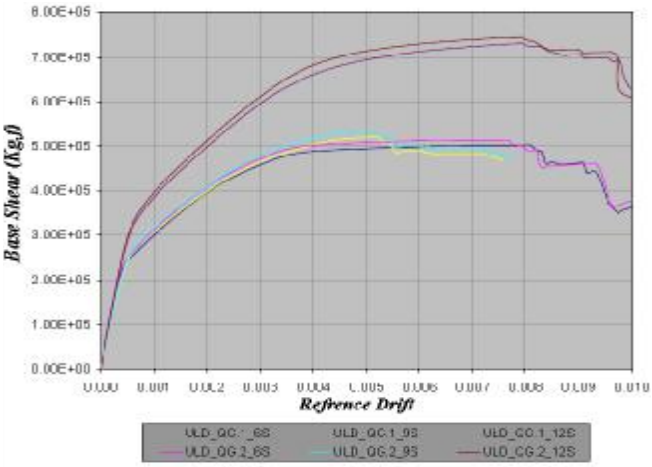

Figure 10. Push-over curves of the ULD load pattern in H2 direction

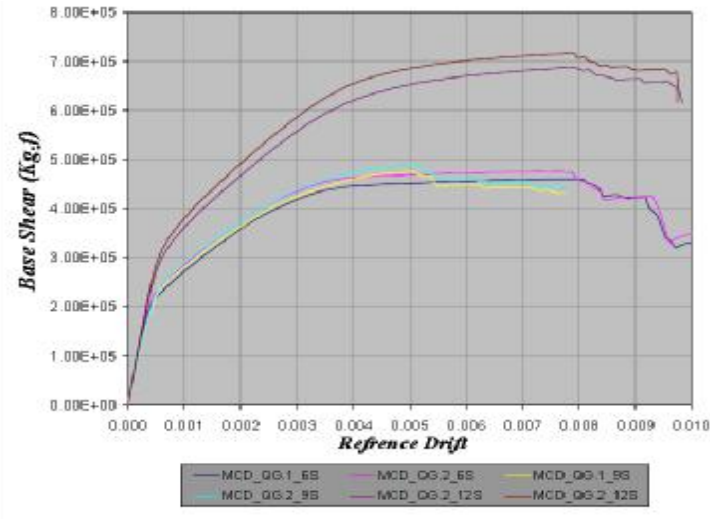

Figure 11. Push-over curves of the MCD load pattern in H2 direction

3.1 Assessment of the performance level

For determining the performance level of the models, improved procedures for equivalent linearization is being used which is explained thoroughly in guideline FEMA 440 [12]. Since the objective of this research is to determine the performance level based on a design earthquake of the ISC [3], the response spectrum is the standard response spectrum of the Iranian Seismic Code for zones of high seismicity with effective peak acceleration (EPA) equal to 0.35g and an assumed site of class B, with T_S = 0.5 s. The obtained results are summarized in Tables 1-9.

Table 1: Target drift, DCR and performance level of 6S model under the load pattern ELF

Direction	**H1**		**H2**	
Gravity load	QG1	QG2	QG1	QG2
Target drift	0.0012	0.0017	0.0010	0.0013
DCR	0.60	0.80	0.35	0.45
Performance level	(IO)	(IO)	(IO)	(IO)

Table 2: Target drift, DCR and performance level of 6S model under the load pattern MCD

Direction	**H1**		**H2**	
Gravity load	QG1	QG2	QG1	QG2
Target drift	0. 0009	0. 0014	0. 0007	0. 0010
DCR	0. 58	0. 58	0. 28	0. 37
Performance level	(IO)	(IO)	(IO)	(IO)

Table 3: Target drift, DCR and performance level of 6S model under the load pattern ULD

Direction	**H1**		**H2**	
Gravity load	Q_{G1}	Q_{G2}	Q_{G1}	Q_{G2}
Target drift	0.0009	0.0011	0.0007	0.0009
DCR	0.55	0.70	0.28	0.34
Performance level	(IO)	(IO)	(IO)	(IO)

Table 4: Target drift, DCR and performance level of 9S model under the load pattern ELF

Direction	**H1**		**H2**	
Gravity load	QG1	QG2	QG1	QG2
Target drift	0.0019	0.0025	0.0019	0.0019
DCR	1.02	1.39	0.94	0.93
Performance level	(LS)	(LS)	(IO)	(IO)

Table 5: Target drift, DCR and performance level of 9S model under the load pattern MCD

Direction	**H1**		**H2**	
Gravity load	Q_{G1}	Q_{G2}	Q_{G1}	Q_{G2}
Target drift	0.0015	0.0022	0.0014	0.0019
DCR	1.05	1.62	0.84	1.11
Performance level	(LS)	(LS)	(IO)	(LS)

Table 6: Target drift, DCR and performance level of 9S model under the load pattern ULD

Direction	**H1**		**H2**	
Gravity load	Q_{G1}	Q_{G2}	Q_{G1}	Q_{G2}
Target drift	0.0014	0.0016	0.0012	0.0017
DCR	1.04	1.23	0.70	1.06
Performance level	(LS)	(LS)	(IO)	(LS)

Table 7: Target drift, DCR and performance level of 12S model under the load pattern ELF

Direction	**H1**		**H2**	
Gravity load	QG1	QG2	QG1	QG2
Target drift	0.0022	0.0025	0.0020	0.0022
DCR	0.74	0.87	0.65	0.69
Performance level	(IO)	(IO)	(IO)	(IO)

Table 8: Target drift, DCR and performance level of 12S model under the load pattern MCD

Direction	**H1**		**H2**	
Gravity load	QG1	QG2	QG1	Q_{G2}
Target drift	0.0015	0.0020	0.0014	0.0017
DCR	0.73	1.03	0.55	0.66
Performance level	(IO)	(LS)	(IO)	(IO)

Table 9: Target drift, DCR and performance level of 12S model under the load pattern ULD

Direction	**H1**		**H2**	
Gravity load	QG1	QG2	QG1	QG2
Target drift	0.0013	0.0017	0.0012	0.0016
DCR	0.65	0.87	0.47	0.61
Performance level	(IO)	(IO)	(IO)	(IO)

4. DISCUSSION

According to tables 1-9, it is concluded that in all of the specimens and load patterns, the demand capacity ratios (DCR) of the load combination Q_{G1} are lower than Q_{G2}. In Figures 6 to 11 it is obvious that the diagrams related to the load combination $Q_{G2,}$ in a similar reference drift, have a higher base shear. According to the amounts of DCR in Tables 1 to 3 it is revealed that the 6S model with a height of 20 m in load combinations Q_{G1} and Q_{G2} and in both directions has the performance level (IO). The amounts of DCR in this model in H1 direction are two times more than H2 direction. In Figures 6 to 11, there is a big difference in the drift of the point where the structure collapses and this difference exists in both H1 and H2 directions and this is an indication of the difference between the ductility ratios of H1 and H_2 directions. Hence, the DCRs in H1 direction are bigger. In Figures 6 to 11, the maximum base shear in both H1 and H2 directions and for all of the load patterns are approximately the same.

The 9S model with a height of 30 m in most of the load patterns and in both directions can not have the (IO) performance level and has a performance level between (IO) and (LS). However, this model can have the proposed performance level of the ISC [3]. In this model, contrary to the 6S model, the DCRs in both directions are approximately the same and with respect to Figures 6 to 11, it is clear that the maximum base shear and the drift of the point where the structure collapses in both directions have a slight difference. The reason for decreasing the performance level of this model, compared to the 6S model, can be understood by noticing these figures. The two models 6S and 9S in H2 direction have a big difference in the drift of the collapse point. Therefore the decrease of the ductility ratio in this model is the main cause for decreasing the performance level. Although in these two

models the maximum base shear and the drift of the collapse point in H1 direction are equal, since the same panels with the same details are used in these two models, and since an increase in the height of the 9S model increases seismic demand of this model, so the performance level of this model decreases.

Regrding Tables 7 to 9 it is noticed that except one DCR, which is equal to 1.03, the rest of the DCRs are below one. Therefore, the performance level of the 12S model with a height of 40 m, which is higher than the maximum height allowed by the ISC [3], is (IO). The reason for the good performance of the 12S model compared to the 9S model is shown in the push-over curves of these models. In these curves, the base shear of the 12S model in the same drift is higher than the base shear of the 9S. This difference is due to an increase in the thickness and bar diameter of the panels of the 12S models. This difference is evident in all of the push-over curves. Also by increasing the height of the model, the flexural behavior of this model improves and so does the performance of this model. In this model, by increasing the ductility ratio and the capacity of the structure at the same time, the performance level increases. Increasing the capacity of the structure has a more important role in improving the performance level of this model.

By comparing the drifts of the models in Tables 1 to 9 and Figures 6 to 11 with the drifts of the performance levels of the guidelines FEMA 273 [2] and FEMA 356 [9], it is obvious that the 0.005 drift is for the (IO) performance level and the 0.01 drift is for the (LS) performance level. Also, with respect to the ISC [3] the amount of the allowable story drift for this structural system based on design earthquake is equal to 0.0071. As a result, this drift indicates that the pre-assumption performance level of the ISC [3] is between (IO) and (LS). According to the push-over curves, most models in the drifts more than 0.007 approach the collapse point. Also according to the small amounts of target drifts in tables 1-9, it is concluded that these structures are brittle.

5. CONCLUDING REMARKS

Since the DCRs resulted from the load combination Q_{G2} were higher than Q_{G1}, it is concluded that the load combination Q_{G2} should be used for performance assessment. In all models, the performance level of the structure in seismic hazard 1 of the Iranian seismic code (ISC) [3] was higher than the pre-assumed performance level of this standard. By increasing the height, the amounts of DCRs related to each direction approached the same amount and caused the model to have the same performance level in both directions.

The performance level of models 6S and 12S in seismic hazard 1 of the ISC [3] was (IO) and the performance level of the 9S model was (LS). This decrease in the performance level of the 9S model is related to the decrease in the ductility ratio and the capacity of the structure in comparison to the other two models. By increasing the height of panel structures, the performance level of these structures are decreased but this decrease is proportional to ductility ratio and capacity.

None of the guidelines FEMA 273 [2], FEMA 356 [9] and ISC [3] provide an exact estimation of the allowable drifts of the panel structures and can not be used in estimating or controlling the performance level of these structures. Due to the very small magnitudes of

the target drifts in the tables above and the drifts of the collapse point in Figures 6 to 11, it is concluded that the considered structures should be classified as brittle. Therefore, the strength based design strategies are more appropriate for these structures. In other words, if these structures are designed according to a strength based design method, they will have good performances and there is no need in controlling their drifts or applying the displacement based design methods to these structures.

REFERENCES

1. Ghobarah A. Performance-based design in earthquake engineering: state of development, *Engineering Structures*, No. 8, **23**(2001) 878–84.
2. FEMA 273. NEHRP Guideline for the Seismic Rehabilitation of Building, *Federal Emergency Management Agency (FEMA)*, Washington D.C, 1997.
3. Iranian code of practice for seismic resistant design of buildings, *Standard No. 2800-05*, 3rd ed., Building and House Research Center (BHRC).
4. UBC, Uniform Building Code - Structural Engineering Design Provisions, *International Conference of Building Officials*, Whittier, California, 1994.
5. Rahul R, Jin L. Pushover analysis of a 19-story concrete shear-wall Building, *Proceedings of the 13th World Conference on Earthquake Engineering*, Vancouver, B.C., Canada, August 1-6, 2004.
6. PERFORM Components and Elements for PERFORM-3D and PERFORM-COLLAPSE, Computers & Structures Inc, Berkeley, USA, 2006.
7. Saenz LP. Equation for the stress-strain curve of concrete in uniaxial and biaxial compression of concrete, *ACI Structural Journal*, No. 9, **61**(1965) 1229-35.
8. Smith GM, Young LY. Ultimate theory in flexure by exponential function, *ACI Structural Journal*, No. 11, **47**(1955) 1013-25.
9. FEMA 356. Pre-standard and Commentary for the Seismic Rehabilitations of Building, *Federal Emergency Management Agency (FEMA)*, Washington D.C, 2000.
10. ACI 318-05. Building Code Requirements for Structural Concrete and Commentary. *ACI 318R-05, American Concrete Institute*, Farming Hills, MI, USA, 2005.
11. Jafari A. A Study on the Seismic Behavior of the Panel Structures, *MSc thesis*, Shahrood University of Technology, 2008.
12. FEMA 440. Improvement of Nonlinear Static Analysis Procedures, *Federal Emergency Management Agency (FEMA)*, Washington D.C., 2005.

«نشریات لاتین»

فنی و مهندسی

ردیف	نام نشریه	اعتبار	آخرین تاریخ تصویب	تاریخ انقضا*	سردبیر
۱	Asian Journal of Civil Engineering (Building and Housing) آسیایی مهندسی عمران ـ مرکز تحقیقات ساختمان و مسکن	علمی ـ پژوهشی	دی ۸۳	مهر ۸۹	علی کاوه
۲	Amirkabir International Journal of Electrical and Electronics Engineering (امیرکبیر سابق) ـ دانشگاه صنعتی امیرکبیر	علمی ـ پژوهشی	اردیبهشت ۷۸	دی ۸۸	سیدکمال‌الدین نیکروش
۳	Amirkabir International Journal of Modeling, Identification, Simulation & Control (امیرکبیر سابق) ـ دانشگاه صنعتی امیرکبیر	علمی ـ پژوهشی	اردیبهشت ۷۸	دی ۸۸	سیدکمال‌الدین نیکروش
۴	Chemical, Polymer and Material Science and Technology, Amirkabir مهندسی شیمی، پلیمر و مواد امیرکبیر (امیرکبیر سابق) ـ دانشگاه صنعتی امیرکبیر	علمی ـ پژوهشی	اردیبهشت ۷۸	دی ۸۸	مرتضی سهرابی
۵	◈Iranian Journal of Biotechnology بیوتکنولوژی ایران ـ مرکز ملی تحقیقات مهندسی ژنتیک و بیوتکنولوژی ایران	علمی ـ پژوهشی	اسفند ۸۲	شهریور ۹۲	عباس صاحبقدم لطفی
۶	Iranian Journal of Chemical Engineering مهندسی شیمی ـ انجمن مهندسی شیمی ایران	علمی ـ پژوهشی	آبان ۸۱	اسفند ۹۰	جعفر توفیقی داریان
۷	Iranian Journal of Electrical and Electronic Engineering مهندسی برق و الکترونیک ـ دانشگاه علم و صنعت	علمی ـ پژوهشی	آذر ۸۱	مهر ۸۹	محمد خلج امیر حسینی
۸	Iranian Journal of Materials Science and Engineering علوم و مهندسی مواد ـ دانشگاه علم و صنعت ـ با همکاری انجمن مهندسی متالوژی و انجمن سرامیک ایران	علمی ـ پژوهشی	آذر ۸۱	اردیبهشت۹۱	پرویز دوامی
۹	Iranian Journal of Mechanical Engineering مهندسی مکانیک ـ انجمن مهندسی مکانیک ایران	علمی ـ پژوهشی	دی ۸۲	مرداد ۹۰	محمدرضا اسلامی
۱۰	Iranian Journal Of Operations Research تحقیق در عملیات ـ انجمن ایرانی تحقیق در عملیات	علمی ـ پژوهشی	مرداد ۸۷	مرداد ۸۸	محمد مدرس یزدی
۱۱	◈◆Iranian Journal of Science & Technology علوم و تکنولوژی ـ دانشگاه شیراز	علمی ـ پژوهشی	خرداد ۸۰	آبان ۹۰	محمود یعقوبی
۱۲	◈Iranian Polymer Journal پلیمر ـ پژوهشگاه پلیمر و پتروشیمی ایران	علمی ـ پژوهشی	دی ۷۸	مهر ۹۱	حمید میرزاده
۱۳	International Journal of Automotive Engineering دانشگاه علم و صنعت ـ با همکاری انجمن مهندسی خودرو ایران	علمی ـ پژوهشی	مرداد ۸۹	اسفند ۸۹	محمدحسن شجاعی‌فرد
۱۴	International Journal of Civil Engineering بین‌المللی مهندسی عمران ـ دانشگاه علم و صنعت ـ با همکاری انجمن مهندسی عمران	علمی ـ پژوهشی	آذر ۸۱	اریبهشت۸۹	محمدحسن بازیار
۱۵	International Journal of Engineering بین‌المللی مهندسی ـ پژوهشگاه مواد و انرژی	علمی ـ پژوهشی	آبان ۷۸	اسفند ۹۰	سید خطیب‌الاسلام صدرنژاد
۱۶	International Journal of Industrial Engineering مهندسی صنایع ـ دانشگاه آزاد اسلامی واحد تهران جنوب	علمی ـ پژوهشی	آبان ۸۷	آبان ۸۹	رسول نورالنساء
۱۷	International Journal of Industrial Engineering and Productional Research بین‌المللی مهندسی صنایع و مدیریت تولید (بین المللی علوم مهندسی سابق) ـ دانشگاه علم و صنعت	علمی ـ پژوهشی	مرداد ۸۰	اسفند ۸۸	سید محمد سید حسینی
۱۸	International Journal of Information and Communication Technology (IJICT) مرکز تحقیقات مخابرات ایران	علمی ـ پژوهشی	بهمن ۸۸	بهمن ۹۰	کامبیز بدیع

◈ این نشریات در پایگاه WOS از موسسه ISI نمایه شده‌اند.

◆ این نشریات در پایگاه JCR از موسسه ISI نمایه شده‌اند و دارای ضریب تأثیر (IF) می‌باشد.

* بر اساس مصوبه مورخ ۸۲/۳/۹ کمیسیون بررسی نشریات علمی کشور تا زمانی که این کمیسیون رأی جدید صادر نکرده است، اعتبار مصوب نشریات علیرغم تاریخ انقضاء باقی است.